Journal Article

Using the parallel stacked mirror model to analytically describe diffraction in the planar volume reflection grating with finite absorption

Brotherton-Ratcliffe, D., Osanlou, A. and Excell, P.

Using the PSM model to analytically describe diffraction in the planar volume reflection grating with finite absorption

David Brotherton-Ratcliffe,[1,2*] Ardie Osanlou,[2] Peter Excell[2]

[1]*Geola Technologies Ltd, Sussex Innovation Centre, Science Park Square, Falmer, East Sussex BN1 9SB, UK*
[2]*Centre for Applied Photonics, Applied Science, Computing and Engineering, Glyndwr University, Mold Road, Wrexham, Wales, LL11 2AW, UK*
**Corresponding author: dbr@geola.co.uk*

Received Month X, XXXX; revised Month X, XXXX; accepted Month X, XXXX; posted Month X, XXXX (Doc. ID XXXXX); published Month X, XXXX

The PSM model of grating diffraction is extended to include a complex refractive index for the case of an unslanted reflection geometry at oblique incidence and for the σ-polarization. The well-known theoretical upper diffraction efficiency limit applicable to reflective absorption gratings described by Kogelnik's coupled-wave theory, is shown to be directly derivable from the PSM model. Analytical formulae for the diffraction efficiency of phase, absorption and mixed harmonic-index gratings are compared with numerical computations using a rigorous coupled wave description. A conventional truncated coupled-wave description, similar to Kogelnik's approach, is also derived from the harmonic-index rigorous coupled wave equations by limiting the propagating modes to a signal and reference wave and by ignoring second order derivatives. At low to moderate average loss the PSM theory is observed to provide a somewhat better fit to the rigorous coupled wave calculations, and this is particularly evident for gratings which are dominated by phase modulation. As the average absorption coefficient is increased, all three models show the diffractive response sharpening around Bragg resonance and the characteristic sideband structure attenuating and then disappearing altogether, giving rise to a broader spectral behavior away from resonance. At high average loss, the truncated coupled wave model is observed to very marginally out-perform PSM. However, overall the PSM model is found to provide an exceedingly good description of the general mixed-phase-absorption unslanted reflection grating with finite average loss.
OCIS codes: (090.0090) Holography; (050.1960) Diffraction Theory.
http://dx.doi/org/10.1364/AO.99.099999

1. Introduction

The Parallel Stacked Mirror (PSM) model (1-6) provides an alternative, and rather more intuitive, analytical model of the diffraction process occurring within lossless planar phase gratings to that offered by the standard coupled-wave theory, which was first introduced by Kogelnik (7).

Recently it has been shown that overall the PSM model constitutes a slightly more accurate model for most lossless reflection phase gratings, whereas for most transmission gratings Kogelnik's theory is observed to generally perform a little better than PSM (6).

The PSM model is based on an application of the concept of Fresnel reflection as first suggested by Rouard in 1937 (8). The grating is decomposed into an infinite series of parallel stacked mirrors, each of which is characterized by an infinitesimal thickness; at each mirror the classical laws of Fresnel transmission and reflection are applied. In this way a reference wave, which illuminates the grating, provokes an infinite sum of secondary "Fresnel" waves, which add to form the overall diffractive response.

The PSM model can be viewed as a differential generalization of the chain matrix method, which is often used in the numerical calculation of the optical properties of stratified media (8-11).

Whereas both PSM and standard coupled wave theory are "approximate" analytical theories, Rigorous Coupled Wave theory (RCW) (12) provides a method of describing the diffractive process to any accuracy required. The theory makes use of a potentially infinite number of coupled waves. The number of waves retained in a calculation depends on the accuracy required, a proportion of which will be evanescent waves. From a practical point of view RCW theory is a numerical technique requiring the solution either of a set of differential equations or the determination of the eigenvalues of a large matrix. As such it cannot offer the advantages of the simple analytic expressions inherent to both standard coupled wave theory and the PSM model.

In the present work we extend the PSM model of diffraction for planar reflection phase gratings to include finite absorption under a σ-polarization. We compare the resulting analytical formulae obtained for the diffractive

efficiency of complex harmonic index gratings with counterparts in standard coupled wave theory. Both analytic theories are then compared with harmonic index rigorous coupled wave calculations.

Whilst the major application that this paper targets is optical diffraction in holographic gratings, the results are also applicable to more general optical gratings. Indeed it has already been shown that the PSM model may be extended (2) to describe diffraction occurring in multiplexed and polychromatic gratings and the results presented herein may easily be generalized to this context. In addition the results of the present study may be utilized to describe particle diffraction from quantum periodic structures as the time independent Schrödinger equation for a harmonic potential is analytically identical to the corresponding Helmholtz equation describing optical diffraction from a harmonic index. Potential applications include the analysis of neutron super-mirrors that have been recorded using holographic techniques (13,14). Finally the results may also be useful in the study of acoustic diffraction from harmonic structures where the transfer matrix approach is well known (15).

2. PSM model of the unslanted grating with finite loss

Following (1) we consider the process of replay of the grating shown in Fig.1. The grating is characterized by a harmonic refractive index

$$n=(n_0+i\chi_0)+\frac{1}{2}(n_1+i\chi_1)\left\{e^{i\mathbf{K}\cdot\mathbf{r}}+e^{-i\mathbf{K}\cdot\mathbf{r}}\right\} \tag{1}$$

where n_0 is the real average refractive index of the grating, n_1 is the real harmonic index modulation, χ_0 is the average imaginary index of the grating, χ_1 is the imaginary harmonic index modulation and $\mathbf{K}$ is the grating vector.

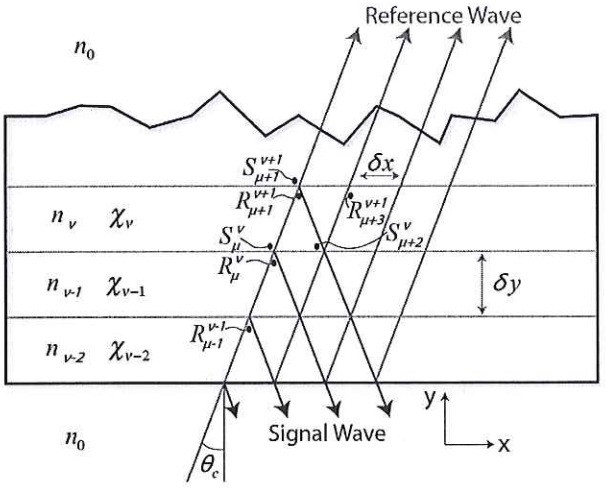

Fig.1 The Replay of an unslanted reflection grating, as treated by the PSM model, showing infinitesimally thick dielectric layers and the Signal and Reference fields present at the index discontinuities.

The grating is illuminated by a wave

$$R=e^{ik_{cx}x+ik_{cy}y} \tag{2}$$

where

$$\mathbf{k}_c=\frac{2\pi n_0}{\lambda_c}\begin{pmatrix}\sin\theta_c\\ \cos\theta_c\end{pmatrix}=\beta\begin{pmatrix}\sin\theta_c\\ \cos\theta_c\end{pmatrix} \tag{3}$$

and where λ_c is the free-space wavelength. The grating vector, $\mathbf{K}$ can be written in terms of a recording angle θ_r and a recording free-space wavelength λ_r

$$\mathbf{K}=2\alpha\beta\cos\theta_r\hat{\mathbf{y}} \tag{4}$$

with

$$\alpha=\lambda_r/\lambda_c \tag{5}$$

The response of the grating to illumination is the generation of a reflected signal wave

$$S=S(y)e^{ik_{kx}x+ik_{ky}y} \tag{6}$$

with

$$\mathbf{k}_i=\beta\begin{pmatrix}\sin\theta_c\\ -\cos\theta_c\end{pmatrix} \tag{7}$$

The grating, as shown in Fig.1, is divided into an infinite number of parallel stacked mirrors. At each such mirror the complex index makes a discontinuous jump and we may apply Fresnel's law to write down expressions for the amplitude transmission and reflection coefficients. Using the notation of superscripts to indicate mirror number in y and subscripts to indicate the quantized x position of a ray intersection, the transmission (t) and reflection (r) amplitude coefficients for the mirror between dielectric regions k and k+1 are respectively

$$\begin{pmatrix}t\\ r\end{pmatrix}_{k,k+1}=\frac{1}{\Omega}\begin{pmatrix}2(n_k+i\chi_k)\sqrt{1-\dfrac{n_0^2}{(n_k+i\chi_k)^2}\sin^2\theta_c}\\ \left\{\begin{matrix}(n_{k+1}+i\chi_{k+1})\sqrt{1-\dfrac{n_0^2}{(n_{k+1}+i\chi_{k+1})^2}\sin^2\theta_c}\\ -(n_k+i\chi_k)\sqrt{1-\dfrac{n_0^2}{(n_k+i\chi_k)^2}\sin^2\theta_c}\end{matrix}\right\}\end{pmatrix} \tag{8}$$

where

$$\Omega = \left\{ \begin{array}{l} (n_{k+1} + i\chi_{k+1}) \sqrt{1 - \dfrac{n_0^{\,2}}{(n_{k+1} + i\chi_{k+1})^2} \sin^2 \theta_c} \\ +(n_k + i\chi_k) \sqrt{1 - \dfrac{n_0^{\,2}}{(n_k + i\chi_k)^2} \sin^2 \theta_c} \end{array} \right\} \tag{9}$$

Here we have assumed that θ_c is the physical angle of incidence. In fact this is an approximation as the introduction of a complex index into Fresnel's law introduces a correction to the physical angle. However this correction is negligible in our case as the imaginary part of the index is always very much smaller than the real part as we shall see below.

Coupled recurrence relations for R and S may now be derived by tracing rays within the grating between mirrors,

$$\begin{array}{l} R_{\mu+1}^{\nu+1} = e^{i\beta(n_\nu + i\chi_\nu)(\sin\theta_x \delta x + \cos\theta_c \delta y)/n_0} R_\mu^\nu t_{\nu-1,\nu} \\ +e^{i\beta(n_\nu + i\chi_\nu)(\sin\theta_x \delta x + \cos\theta_c \delta y)/n_0} S_\mu^\nu r_{\nu,\nu-1} \end{array} \tag{10}$$

and

$$\begin{array}{l} S_{\mu+1}^{\nu-1} = e^{i\beta(n_\nu + i\chi_\nu)(\sin\theta_x \delta x + \cos\theta_c \delta y)/n_0} S_\mu^\nu t_{\nu,\nu-1} \\ +e^{i\beta(n_\nu + i\chi_\nu)(\sin\theta_x \delta x + \cos\theta_c \delta y)/n_0} R_\mu^\nu r_{\nu-1,\nu} \end{array} \tag{11}$$

Using Taylor expansions for R, S, n and χ

$$\begin{array}{l} R_{\mu+1}^{\nu+1} = R_\mu^\nu + \dfrac{\partial R_\mu^\nu}{\partial x}\delta x + \dfrac{\partial R_\mu^\nu}{\partial y}\delta y + \ldots \\ S_{\mu+1}^{\nu-1} = R_\mu^\nu + \dfrac{\partial S_\mu^\nu}{\partial x}\delta x - \dfrac{\partial S_\mu^\nu}{\partial y}\delta y + \ldots \end{array} \tag{12}$$

$$\begin{array}{l} n_{\nu-1} = n_\nu + \dfrac{\partial n_\nu}{\partial x}\delta y + \ldots \\ \chi_{\nu-1} = \chi_\nu + \dfrac{\partial \chi_\nu}{\partial x}\delta y + \ldots \end{array} \tag{13}$$

Letting $\delta x, \delta y \to 0$ and making the approximation of a constant ray direction, we then arrive at a differential description

$$\frac{1}{\beta}\begin{pmatrix} \mathbf{k}_c \cdot \nabla R \\ \mathbf{k}_i \cdot \nabla S \end{pmatrix} = \begin{pmatrix} \upsilon - \rho & -\rho \\ \rho & \upsilon + \rho \end{pmatrix}\begin{pmatrix} R \\ S \end{pmatrix} \tag{14}$$

where

$$\begin{array}{l} \upsilon = \dfrac{i\beta}{n_0}(n + i\chi) \\ \rho = \dfrac{1}{2(n + i\chi)\cos\theta_c}\left[\dfrac{\partial n}{\partial y} + i\dfrac{\partial \chi}{\partial y}\right] \end{array} \tag{15}$$

We now make the transformations

$$\begin{array}{l} R \to R'(y) e^{i\beta(\cos\theta_c y + \sin\theta_c x)} \\ S \to S'(y) e^{i\beta(-\cos\theta_c y + \sin\theta_c x)} \end{array} \tag{16}$$

and

$$\begin{array}{l} < R' >= \overline{R} \\ < S' >= \overline{S} \end{array} \tag{17}$$

where triangular brackets indicate an average over several cycles of the harmonic functions they operate on. The first component of equation (14) may then be written as

$$\begin{array}{l} \dfrac{1}{\alpha}\dfrac{\cos^2\theta_c}{\cos\theta_r}\dfrac{d\overline{R}}{dy} = -\left\{\dfrac{\beta}{\alpha}\left(\dfrac{\chi_0}{n_0}\right)\dfrac{\cos\theta_c}{\cos\theta_r}\right\}\overline{R} \\ -\left\{\dfrac{1}{2} i\beta \dfrac{\left[(n_0 n_1 + \chi_0\chi_1) + i(n_0\chi_1 - n_1\chi_0)\right]}{(n_0^2 + \chi_0^2)}\right\} \times \\ e^{2i\beta(\alpha\cos\theta_r - \cos\theta_c)y}\overline{S} \end{array} \tag{18}$$

Introducing a pseudo-field

$$\hat{S} = e^{2i\beta(\alpha\cos\theta_r - \cos\theta_c)y}\overline{S} \tag{19}$$

we arrive at the simple differential equation

$$c_R \frac{d\overline{R}}{dy} + \overline{\alpha}\overline{R} + i\hat{\kappa}\hat{S} = 0 \tag{20}$$

where

$$\begin{array}{l} c_R = \dfrac{1}{\alpha}\dfrac{\cos^2\theta_c}{\cos\theta_r} \\ \overline{\alpha} = \dfrac{\chi_0\beta}{\alpha n_0}\dfrac{\cos\theta_c}{\cos\theta_r} \\ \hat{\kappa} = \dfrac{1}{2}\beta\dfrac{\left[(n_0 n_1 + \chi_0\chi_1) + i(n_0\chi_1 - n_1\chi_0)\right]}{(n_0^2 + \chi_0^2)} \\ \quad \approx \dfrac{\beta}{2n_0}(n_1 + i\chi_1) \end{array} \tag{21}$$

In exactly the same manner, the second component of equation (14) leads to

$$c_S \frac{d\hat{S}}{dy} + (\overline{\alpha} + i\vartheta)\hat{S} + i\hat{\kappa}\overline{R} = 0 \tag{22}$$

where

$$c_S = -\frac{1}{\alpha}\frac{\cos^2\theta_c}{\cos\theta_r}$$
$$\vartheta = 2\beta(1-\frac{\cos\theta_c}{\alpha\cos\theta_r})\cos^2\theta_c \tag{23}$$

Equations (20) and (22) are of course none other than Kogelnik's equations (7) for a lossy planar grating with harmonic permittivity. However the coefficients given in equation (21) and equation (23) are different.

Equations (20) and (22) may be solved analytically given the boundary conditions appropriate for a reflection geometry

$$\overline{R}(0) = 1$$
$$\hat{S}(d) = 0 \tag{24}$$

The reflected signal field at the front of the grating is given by

$$\hat{S}(0) = -2ic_R\hat{\kappa}\,/$$
$$\left\{(c_R - c_S)\overline{\alpha} + ic_R\vartheta - \left[\sqrt{\{\overline{\alpha}(c_S - c_R) - ic_R\vartheta\}^2 - 4c_Rc_S\hat{\kappa}^2}\right]\coth(\frac{\Omega d}{2c_Sc_R})\right\} \tag{25}$$
$$= -2i\hat{\kappa}\,/$$
$$\left\{2\overline{\alpha} + i\vartheta + \left[\sqrt{\{2\overline{\alpha} + i\vartheta\}^2 + 4\hat{\kappa}^2}\right]\coth(\frac{\Omega d}{2c_R^2})\right\}$$

where

$$\Omega = \sqrt{\left(\{c_R + c_S\}\overline{\alpha} + ic_R\vartheta\right)^2 - 4c_Rc_S\left(\overline{\alpha}^2 + i\overline{\alpha}\vartheta + \hat{\kappa}^2\right)} \tag{26}$$
$$= c_R\sqrt{4\left(\overline{\alpha}^2 + i\overline{\alpha}\vartheta + \hat{\kappa}^2\right) - \vartheta^2}$$

The diffraction efficiency is then given by

$$\eta_\sigma = \left|\frac{c_S}{c_R}\right|\hat{S}(0)\hat{S}^*(0) = \hat{S}(0)\hat{S}^*(0) \tag{27}$$

3. Rigorous coupled wave theory for the harmonic index grating with finite loss

The Helmholtz equation provides a rigorous description of diffraction from the grating and may be written for the case of the σ-polarization as

$$\frac{\partial^2 u}{\partial x^2} + \frac{\partial^2 u}{\partial y^2} - \gamma^2 u = 0 \tag{28}$$

where u is the transverse electric field (in the z-direction – see Fig.1) and

$$\gamma^2 = -(\beta^2 + 2\kappa^2 - 2i\hat{\alpha}\beta) - 2\beta\kappa\left[e^{iK\cdot r} + e^{-iK\cdot r}\right] - \kappa^2\left[e^{2iK\cdot r} + e^{-2iK\cdot r}\right] \tag{29}$$

with

$$\kappa = \frac{\pi\{n_1 + i\chi_1\}}{\lambda_c} = \frac{\beta}{2n_0}\{n_1 + i\chi_1\}$$
$$\hat{\alpha} = -\frac{\beta\chi_0}{n_0}(1 + i\frac{\chi_0}{2n_0}) \tag{30}$$

Following (6) the rigorous coupled wave equations can then be written

$$\frac{d^2\hat{u}_l(y)}{dy^2} + 2i(k_y + lK_y)\frac{d\hat{u}_l(y)}{dy} = \left\{\begin{matrix}(k_x + lK_x)^2 + (k_y + lK_y)^2 \\ -(\beta^2 + 2\kappa^2) + 2i\hat{\alpha}\beta\end{matrix}\right\}\hat{u}_l(y) - 2\beta\kappa\left\{\hat{u}_{l-1}(y) + \hat{u}_{l+1}(y)\right\} - \kappa^2\left\{u_{l-2}(y) + u_{l+2}(y)\right\} \tag{31}$$

where

$$u(x,y) = \sum_{l=-\infty}^{\infty} u_l(y)e^{i(k_x + lK_x)x} \tag{32}$$

and

$$u_l(y) = \hat{u}_l(y)e^{i(k_y + lK_y)y} \tag{33}$$

Outside the grating the refractive index is assumed to be real-valued and equal to n_0. The boundary conditions are determined by demanding continuity of the tangential electric and magnetic fields. At the front surface of the grating the boundary conditions are

$$\left.\begin{matrix}\hat{u}_0'(y=0) = 2ik_y\{1 - \hat{u}_0(y=0)\} & l = 0 \\ \hat{u}_l'(y=0) + i(k_y + lK_y)\hat{u}_l(y=0) = & \forall l \neq 0 \\ -i\left\{\sqrt{\beta^2 - (k_x + lK_x)^2}\right\}\hat{u}_l(y=0) & \end{matrix}\right\} \tag{34}$$

and at the rear surface

$$\hat{u}_l'(y=d)+i(k_y+lK_y)\hat{u}_l(y=d)$$
$$=i\left\{\sqrt{\beta^2-(k_x+lK_x)^2}\right\}\hat{u}_l(y=d) \tag{35}$$

The flow of energy across the front surface of the grating is described by the Poynting vector

$$\mathbf{S}=\int_{-\infty}^{\infty}(\mathbf{E}\times\mathbf{H}).\hat{\mathbf{y}}dx=$$
$$\int_{-\infty}^{\infty}\Re e(u(x,y))\Im m\left\{i\frac{du(x,y)}{dy}\right\}dx \tag{36}$$

and accordingly it is clear that we must define the diffraction efficiency as

$$\eta_{-l}=\frac{\sqrt{\beta^2-(k_x+lK_x)^2}}{k_y}\hat{u}_l\hat{u}_l^*$$
$$\eta_0=(\hat{u}_0-1)(\hat{u}_0^*-1) \tag{37}$$

Equations (31) subject to boundary conditions (34) and (35) may be solved by a state-space method proposed by Moharam and Gaylord (11) which is also explicitly described in (6).

4. Truncated coupled wave theory

Following Kogelnik (7) we may derive an analytic coupled wave theory from the rigorous coupled wave equations describing the harmonic index grating by ignoring second order derivatives and truncating the mode expansion to a single reference and signal wave. For clarity, this procedure, when applied to the rigorous coupled wave equations describing an harmonic permittivity grating, leads directly to Kogelnik's equations (7).

Applying this procedure to equation (31) yields

$$2ik_y\frac{dR(y)}{dy}=\begin{Bmatrix}(k_x)^2+(k_y)^2\\-(\beta^2+2\kappa^2)+2i\hat{\alpha}\beta\end{Bmatrix}R(y)$$
$$-2\beta\kappa S(y)$$
$$2i(k_y-K_y)\frac{dS(y)}{dy}=\begin{Bmatrix}(k_x-K_x)^2+(k_y-K_y)^2\\-(\beta^2+2\kappa^2)+2i\hat{\alpha}\beta\end{Bmatrix}S(y) \tag{38}$$
$$-2\beta\kappa R(y)$$

These equations may then be written in canonical form as

$$\tilde{c}_R\frac{dR}{dy}+\tilde{\alpha}R+i\kappa S=0$$
$$\tilde{c}_S\frac{dS}{dy}+(\tilde{\alpha}+i\tilde{\vartheta})S+i\kappa R=0 \tag{39}$$

where

$$\tilde{c}_R=-\cos\theta_e$$
$$\tilde{c}_S=-(\cos\theta_e-2\alpha\cos\theta_r)$$
$$\tilde{\alpha}=\hat{\alpha}+\frac{i\kappa^2}{\beta} \tag{40}$$
$$\tilde{\vartheta}=2\alpha\beta\cos\theta_r(\cos\theta_e-\alpha\cos\theta_r)$$

Note that equations (39) are none other than equations (20) and (22). However the coefficients given in equations (40) differ from those of equations (21) and (23). This difference in coefficients constitutes the main practical difference between the PSM model and the truncated coupled wave model. Note also that Kogelnik's equations (7), which describe a complex harmonic permittivity grating as opposed to a complex harmonic index grating, differ from equations (39) and (40) only in the alpha coefficient which is then given by

$$\tilde{\alpha}=\hat{\alpha} \tag{41}$$

Using the reflection boundary conditions

$$R(0)=1$$
$$S(d)=0 \tag{42}$$

we may, as before, write down an analytic expression for the amplitude of the signal wave at the front boundary of the grating

$$\hat{S}(0)=-2i\tilde{c}_R\kappa\,/$$
$$\left\{(\tilde{c}_R-\tilde{c}_S)\tilde{\alpha}+i\tilde{c}_R\tilde{\vartheta}-\left[\sqrt{\{\tilde{\alpha}(\tilde{c}_S-\tilde{c}_R)-i\tilde{c}_R\tilde{\vartheta}\}^2-4\tilde{c}_R\tilde{c}_S\kappa^2}\right]\coth\left(\frac{\Omega d}{2\tilde{c}_S\tilde{c}_R}\right)\right\} \tag{43}$$

where

$$\Omega=\sqrt{\left(\{\tilde{c}_R+\tilde{c}_S\}\tilde{\alpha}+i\tilde{c}_R\tilde{\vartheta}\right)^2-4\tilde{c}_R\tilde{c}_S\left(\tilde{\alpha}^2+i\tilde{\alpha}\tilde{\vartheta}+\kappa^2\right)} \tag{44}$$

The diffraction efficiency is then given by

$$\eta_\sigma=\left|\frac{\tilde{c}_S}{\tilde{c}_R}\right|S(0)S^*(0) \tag{45}$$

5. Analytic solutions at Bragg resonance

The diffractive efficiency of unslanted mixed phase-absorption reflection gratings with finite loss may be expressed using the same analytic form under both the PSM model and the truncated coupled-wave model

$$\eta_\sigma = \frac{|\kappa_B|^2 \left| \sinh\left[\frac{d\sqrt{\alpha_B^{\,2} + \kappa_B^{\,2}}}{c_{BR}} \right] \right|^2}{\left| \sqrt{\alpha_B^{\,2} + \kappa_B^{\,2}} \cosh\left[\frac{d\sqrt{\alpha_B^{\,2} + \kappa_B^{\,2}}}{c_{BR}} \right] + \alpha_B \sinh\left[\frac{d\sqrt{\alpha_B^{\,2} + \kappa_B^{\,2}}}{c_{BR}} \right] \right|^2} \quad (46)$$

In the case of PSM the coefficients are given by

$$\begin{aligned} c_{BR} &= -c_{BS} = \cos\theta_c \\ \alpha_B &= \frac{\chi_0 \beta}{n_0} \\ \kappa_B &= \frac{1}{2}\beta \frac{[(n_0 n_1 + \chi_0 \chi_1) + i(n_0 \chi_1 - n_1 \chi_0)]}{(n_0^2 + \chi_0^2)} \end{aligned} \quad (47)$$

and in the case of the truncated coupled wave theory,

$$\begin{aligned} c_{BR} &= -c_{BS} = -\cos\theta_c \\ \alpha_B &= \hat{\alpha} + \frac{i\kappa_B^{\,2}}{\beta} = -\frac{\beta\chi_0}{n_0}\left(1 + i\frac{\chi_0}{2n_0}\right) + \frac{i\beta}{4n_0^{\,2}}\{n_1 + i\chi_1\}^2 \\ \kappa_B &= \frac{\beta}{2n_0}\{n_1 + i\chi_1\} \end{aligned} \quad (48)$$

When $\chi_0 << n_0$ and $n_1 << n_0$, which is very often the case, these coefficients become identical,

$$\begin{aligned} c_{BR} &= -c_{BS} = -\cos\theta_c \\ \alpha_B &= -\frac{\beta\chi_0}{n_0} \\ \kappa_B &= \frac{\beta}{2n_0}\{n_1 + i\chi_1\} \end{aligned} \quad (49)$$

Note that the transformation $c_{BR} \to -c_{BR}$ and $\alpha_B \to -\alpha_B$ leaves η_σ invariant. Note also that when $\chi_0 = \chi_1 = 0$ we retrieve Kogelnik's well-known formula (7)

$$\eta_\sigma = \tanh^2\left(\frac{\kappa_B d}{\sqrt{c_{BR} c_{BS}}}\right) \quad (50)$$

6. Phase gratings with finite average loss

Kogelnik (7) defines a parameter, D_0 which is similar to the photographic density

$$D_0 \equiv \frac{\mu_0 c \sigma_0 d}{2\cos\theta_c \sqrt{\varepsilon_0}} \quad (51)$$

Here μ_0 is the vacuum permeability, c is the velocity of

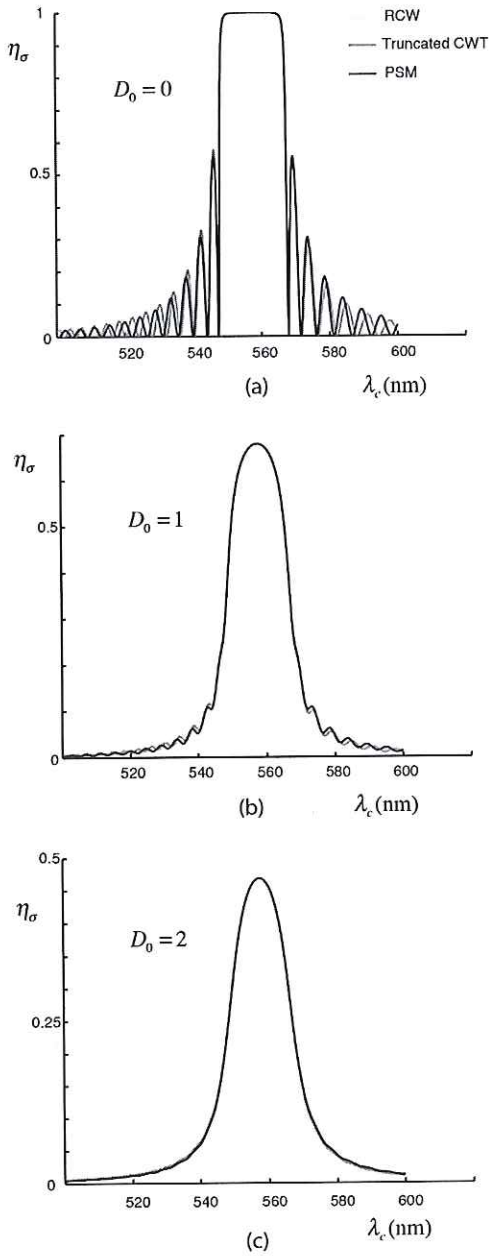

Fig.2 Diffraction efficiency versus replay wavelength showing the effect of increasing the average loss, D_0. The graphs pertain to gratings recorded at an (internal) incidence angle of 20 degrees and replayed at 10 degrees. The recording wavelength is 532nm and the grating has a thickness of 20 microns. The index modulation is real with a value of n_1 of 0.045. n_0=1.5. On each plot there are three lines corresponding to PSM (black), Rigorous Coupled Wave theory (green) and Truncated Coupled Wave theory (red).

light, ε_0 is the vacuum permittivity and σ_0 is the average grating conductivity. In the case of visible wavelengths and for grating thicknesses less than 100 microns we may use the approximation $\chi_0 << n_0$ leading to the simplified expression

$$D_0 \approx \frac{2\pi d\chi_0}{\lambda_c \cos\theta_c} \tag{52}$$

In Fig.2 we plot the diffractive efficiency versus replay wavelength of typical reflective gratings having different values of D_0 and a zero value of χ_1 as calculated by the PSM model (equations (25)-(27)), truncated coupled wave theory (equations (43)-(45)) and rigorous coupled wave theory (equation (37) with $l = -1$). The RCW calculation uses 7 modes in total.

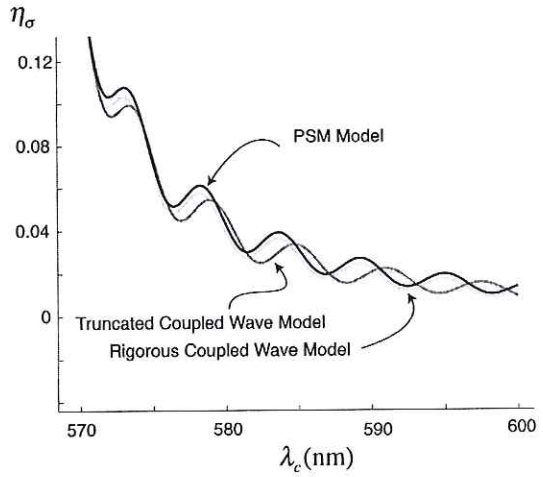

Fig.3. Magnified section of Fig.2(b) showing the typically better fit obtainable with PSM to the rigorous coupled wave solution than that offered by the truncated coupled wave approach.

Clearly the PSM model provides a somewhat better description of the diffractive behavior at low to moderate values of D_0 as compared to the truncated coupled wave theory. This is particularly true in relation to the distinctive sideband structure (see Fig.3). However, as D_0 becomes large, the sideband structure starts to diminish before finally disappearing. As D_0 further increases the truncated coupled wave theory starts to slightly out-perform the PSM model in certain cases but the difference is very minimal. An identical behavior is also shown in plots of the diffractive efficiency versus replay angle.

7. Absorption gratings with finite average loss

Following Kogelnik (7) we introduce a density parameter for the harmonic absorption coefficient of the grating

$$D_1 \quad \frac{2\pi d\chi_1}{\lambda_c \cos\theta_c} \tag{53}$$

Using Equations (46) and (49) and putting $D_0 = D_1$, which represents the deepest possible modulation for an absorption grating, we retrieve Kogelnik's upper diffraction limit

$$\eta_\sigma = \frac{1}{4 + 4\sqrt{3}\coth\left[\frac{D_0\sqrt{3}}{2}\right] + 3\coth^2\left[\frac{D_0\sqrt{3}}{2}\right]}$$

$$= \frac{1}{7 + 4\sqrt{3}} \quad as \ D_0 \to \infty \tag{54}$$

$$0.071797$$

This result is then derivable either through truncated coupled wave theory or through the PSM approach. A more general formula (see Fig 4), valid for arbitrary average and harmonic absorption, is

$$\eta_\sigma = \frac{\gamma^2 \sinh\left[\frac{1}{2}D_0\sqrt{4-\gamma^2}\right]^2}{\left(\sqrt{4-\gamma^2}\cosh\left[\frac{1}{2}D_0\sqrt{4-\gamma^2}\right] + 2\sinh\left[\frac{1}{2}D_0\sqrt{4-\gamma^2}\right]\right)^2} \tag{55}$$

where

$$\gamma \equiv D_1 / D_0 \tag{56}$$

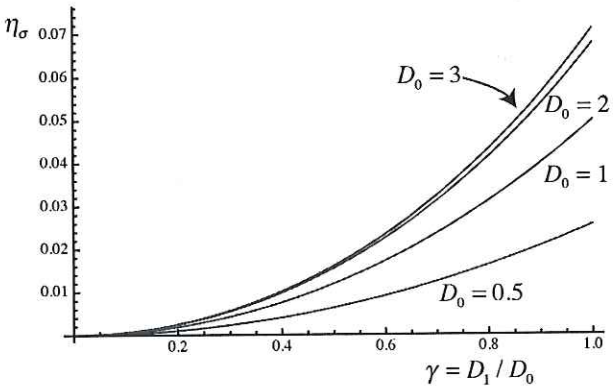

Fig.4. Diffraction efficiency at Bragg resonance for an unslanted absorption grating versus the ratio of harmonic to average loss for various values of average loss. This graph is calculated using equations (55) and (56) which are a result of both the PSM model and Truncated Coupled Wave Theory.

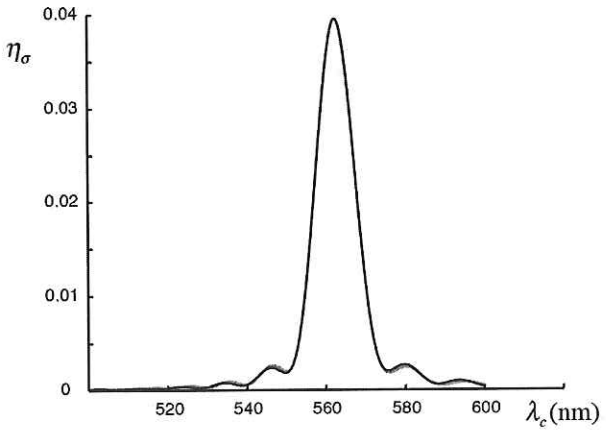

Fig.5. Diffraction efficiency versus replay wavelength for an unslanted absorption grating of thickness 10 microns with D_0 and D_1 equal to 0.75. Recording Wavelength 532nm. Recording incidence angle 35 degrees. Replay incidence angle 30 degrees. n_0=1.5. Green line indicates rigorous coupled wave calculation. Red line indicates truncated coupled wave model. Black line represents the PSM model.

To compare the performance of the PSM model and the truncated coupled wave approach we plot in Fig.5 the diffraction efficiency versus replay wavelength for a typical ten micron thick absorption grating with D_0=D_1=0.75. Here we compare the PSM model (equations (25)-(27)), the truncated coupled wave theory (equations (43)-(45)) and rigorous coupled wave theory (37) with $l=-1$. As with phase gratings we once again see that characteristic sidebands are clearly present. An enlargement of these structures (see Fig.6) shows that the PSM theory is, as before, slightly closer to the rigorous coupled wave calculation when compared to truncated coupled wave theory. However at D_0=D_1=3.0, representing the case of very large absorption, we observe that the sidebands vanish and now truncated coupled wave theory is seen to slightly outperform PSM.

8. Mixed gratings with finite average loss

In Fig.7 we plot the diffractive efficiency versus replay wavelength for the case of Fig.5 but where now a finite value of n_1 is also included. This is a mixed phase-absorption grating. The PSM model is again seen to give a slightly better description of the diffractive structure for low to moderate loss.

9. Discussion

In this paper we have extended the PSM model (1-6) of diffraction from planar gratings to include a complex index of refraction for the case of zero grating slant, the σ-polarization and a reflection geometry. This has allowed us to derive analytical expressions for the diffractive efficiency of phase gratings with finite background loss, absorption gratings and mixed phase-absorption gratings. In order to ascertain the performance of the PSM model we have compared it with truncated coupled wave theory (7) and rigorous coupled wave theory (12). The major result is that the PSM analytic model provides an excellent description of the diffraction process in all three cases studied – reflective phase gratings with finite background loss, reflective absorption gratings and mixed reflective phase-absorption gratings.

The behavior of PSM relative to truncated coupled wave theory largely mirrors the case of a real index studied in (1). In particular the characteristic diffractive sideband structure appears better described by the PSM model. However in cases of very high background loss, this structure averages out and disappears, and in such cases truncated coupled wave theory produces a slightly closer result to rigorous coupled wave theory. Another observation we could make is that thinner gratings tend to be modeled somewhat better using PSM. This is no doubt largely to do with a better modeling by PSM of the second order derivatives in equation (31) and also the averaging process defined in equation (17), which is fundamental to PSM and which requires very few cycles to produce effective results, particularly if the grating thickness represents an exact number of waves.

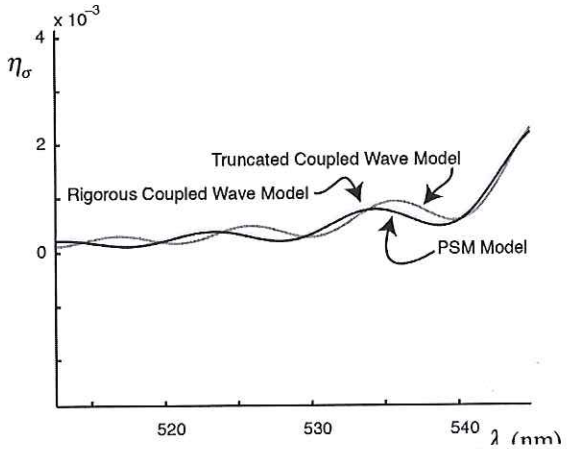

Fig.6 Magnified section of Fig.5 showing the typically better fit obtainable (for absorption gratings) with PSM to the rigorous coupled wave solution than that offered by the truncated coupled wave approach.

The major application of this work is in describing optical diffraction occurring in holographic gratings. However PSM may also be applied to particle wave diffraction where the concept of "Fresnel" reflection is well known (16). Potential applications include the analysis of neutron super-mirrors that have been recorded using optical holographic techniques (13,14). Our results may also be useful in the study of acoustic diffraction from harmonic structures where once again the acoustic equations reduce to the same equations governing optical diffraction (15).

Finally we should comment on the computational use of our results. In particular we have presented analytic formulae that may be used to practically and easily calculate diffraction efficiencies. Although we are unable to say that these analytic results of the PSM theory always

constitute a better model than those of the truncated coupled wave theory, in many cases this is so. Where exact computation is required an "exact" method such as rigorous coupled wave theory provides the preferred

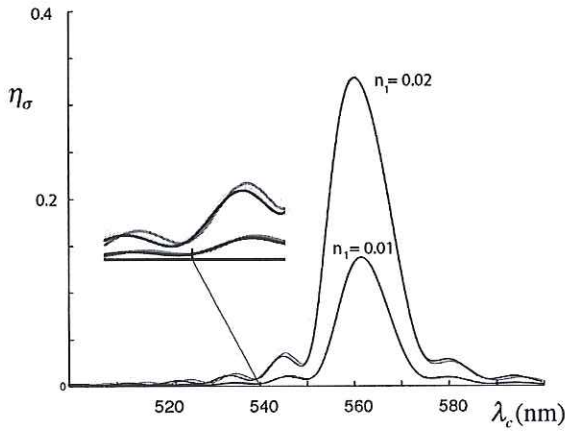

Fig.7 Mixed phased absorption grating. The plot is identical to Fig.6 except that a finite real harmonic index has been added. Green line indicates rigorous coupled wave calculation. Red line indicates truncated coupled wave model. Black line represents the PSM model.

computational technique. However this is always at a far greater cost in floating-point operations and in certain circumstances the extra accuracy available through such exact methods is simply not warranted when the analytic expressions presented here require far less computational resources.

10. Conclusion

The PSM model of grating diffraction has been extended to include a complex refractive index for the case of an unslanted reflection geometry at oblique incidence and for the σ-polarization. The well-known theoretical upper diffraction efficiency limit applicable to reflective absorption gratings described by Kogelnik's coupled-wave theory, is shown to be directly derivable from the PSM model. Analytical formulae for the diffraction efficiency of phase, absorption and mixed harmonic-index gratings have been compared with numerical computations using a rigorous coupled wave description. A conventional truncated coupled-wave description, similar to Kogelnik's approach, has also been derived from the harmonic-index rigorous coupled wave equations by limiting the propagating modes to a signal and reference wave and by ignoring second order derivatives.

At low to moderate average loss the PSM theory is observed to provide a somewhat better fit to the rigorous coupled wave calculations, and this is particularly evident for gratings which are dominated by phase modulation. As the average absorption coefficient is increased, all three models show the diffractive response sharpening around Bragg resonance and the characteristic sideband structure attenuating and then disappearing altogether, giving rise to a broader spectral behavior away from resonance. At high average loss the truncated coupled wave model is observed to very marginally out-perform PSM. However, overall the PSM model is found to provide an exceedingly good description of the general mixed-phase-absorption unslanted reflection grating with finite average loss.

References

1. D.Brotherton-Ratcliffe, "A treatment of the general volume holographic grating as an array of parallel stacked mirrors," J. Mod Optic. **59**, 1113-1132 (2012).
2. D.Brotherton-Ratcliffe, "Analytical treatment of the polychromatic spatially multiplexed volume holographic grating," Appl. Opt. **51**, 7188-7199 (2012).
3. D.Brotherton-Ratcliffe, "A new type of coupled wave theory capable of analytically describing diffraction in polychromatic spatially multiplexed holographic gratings," Journal of Physics: Conference Series **415** (2013) 012034 doi:10.1088/1742-6596/415/1/012034.
4. H.Bjelkhagen and D.Brotherton-Ratcliffe, "Ultra-realistic Imaging – advanced techniques in analogue and digital colour holography", Book, 638 pages, full colour, Taylor and Francis□ISBN-10: 1439827990 | ISBN-13: 978-1439827994, (2012).
5. D.Brotherton-Ratcliffe, "Understanding diffraction in volume gratings and holograms", chapter 1 of "Holography - Basic Principles and Contemporary Applications", book edited by Emilia Mihaylova, INTECH, ISBN 978-953-51-1117-7, May 29, (2013).
6. D.Brotherton-Ratcliffe, L. Shi. A.Osanlou, P.Excell, "A Comparative Study of the Accuracy of the PSM and Kogelnik Models of Diffraction in Reflection and Transmission Holographic Gratings", Optics Express, Vol. 22 Issue 26, pp.32384-32405, (2014).
7. H.Kogelnik, "Coupled wave theory for thick hologram gratings," Bell Syst. Tech. J. **48**, 2909-2947 (1969).
8. M.P.Rouard, "Etudes des propriétés optiques des lames métalliques très minces," Ann. Phys. (Paris) Ser. II **7**, 291-384 (1837).
9. F.Abeles, "Recherches sur la propagation des ondes électromagnétiques sinusoïdales dans les milieux stratifiés, Application aux couches minces," Ann. Phys. (Paris) **5**, 596-640 (1950).
10. O.S.Heavens, "Optical Properties of thin films," Reports on Progress in Physics, Vol XXIII, (1960) p1.
11. M.G.Moharam and T.K.Gaylord, "Chain-matrix analysis of arbitrary-thickness dielectric reflection gratings," J. Opt. Soc. Am. **72**, 187-190 (1982).
12. M.G.Moharam and T.K.Gaylord, "Rigorous coupled wave analysis of planar grating diffraction," J. Opt. Soc. Am. **71**, 811-818 (1981).
13. M.Fally *et al*, Diffraction gratings for neutrons from polymers and holographic polymer-dispersed liquid crystals 2009 *J. Opt. A: Pure Appl. Opt.* **11** 024019
14. J.Klepp et al, "Holographic Gratings for slow-neutron optics", *Materials*, *5*, 2788-2815;doi:10.3390/ma5122788 (2012)
15. M.Abid et al, "Acoustic Response of a Multilayer Panel with Viscoelastic Material", International Journal of Acoustics and Vibration, Vol. 17, No.2, pp82-89 (2012)
16. J.Lekner, "Theory of Reflection – Developments in electromagnetic theory and applications", Martinus Nijhhoff publishers, IBSN 978-90-481-8299-2, (1987)